Potential of Hydraulic Waste Heat Recovery for Cabin Comfort

Fabian Lagerstedt[1,2], Samuel Kärnell[2], Marcus Rösth[3], and Liselott Ericson[2]

[1]Huddig AB, Hudiksvall, Sweden
E-mail: fabian.lagerstedt@huddig.se, samuel.karnell@liu.se, marcus@rosth.com, liselott.ericson@liu.se
[2]Division of Fluid and Mechatronic Systems, Linköping University, Linköping, Sweden
[3]Hudiksvalls Hydraulikkluster, Hudiksvall, Sweden

Abstract

Electrification of mobile machines requires focus on reducing unnecessary energy consumption, which is essential to avoid the need for oversized energy storage. Waste heat recovery of already existing heat flows in the vehicle, such as the working hydraulic system, is a promising way of reducing the energy consumption needed for keeping the cabin warm in the winter. This paper presents a model of a heat recovery concept from the working hydraulic system to the cabin, different from the ones typically seen in the literature. The model is created with the open-source tool OpenModelica together with the DLR Thermofluid Stream library. Focus of the model was to analyze how the dynamic characteristics of the working hydraulic system affects the cabin temperature, and to evaluate the waste heat performance. The results show that the cabin temperature fluctuates close to detectable variations without any interference of active temperature control, and also indicates promising cabin heating performance even under lower operation intensities.

Keywords: Heat recovery, working hydraulics, ITMS, mobile machine, electric vehicle

1 Introduction

Transitioning from internal combustion engine (ICE) and diesel hybrid into fully electric mobile machines typically means losing a major heat source and energy storage. Increasing the energy efficiency of the vehicle is one way to tackle these issues. One widespread issue with electric vehicles is high energy consumption for cabin heating during the winter, which has been addressed recent years by implementation of waste heat recovery and heat pump systems in integrated thermal management system architectures [1] [2].

Due to the lack of available waste heat on electric passenger to heat the cabin alone, waste heat recovery solutions on cars involves boosting the performance of a heat pump [3]. For mobile machines the waste heat conditions are different. From previous work [4] it was concluded that the available waste heat exceeds the cabin demand during high-utility excavating and transport cycles, shown in fig. 1. Based on those results, waste heat recovery from the working hydraulic system gained attention for further studies.

In contrast to other fluid circuits on a vehicle, the working hydraulic system in a mobile machine shows highly dynamic characteristics. This can cause challenges in the context of heat recovery. Especially when the recovered heat is targeted to a cabin, where arbitrary temperature fluctuations is not considered desirable. Battistel et.al. showed by experiments in climate chambers that a temperature deviation as small as 0.38°C in any direction from the base temperature 24°C was detected with 75% accuracy, and that +0.8°C and –0.91°C was detected with 100% accuracy [5].

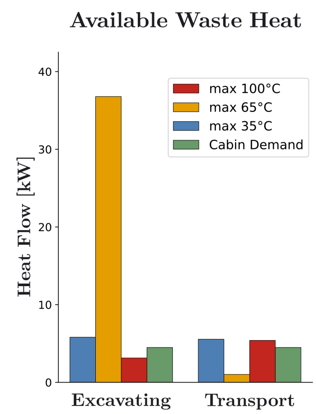

Figure 1: Thermal load or available waste heat during high-utility excavating or transportation in –15°C, divided into temperature categories—compared with cabin heating demand in green. Originates from previous work [4].

Heat recovery from working hydraulic systems has recently been investigated by [6], where the dynamic challenge was specifically addressed. They used an Organic Rankine Cycle to convert the waste heat into electric power, and the results showed that the flow fluctuations did not have as high impact as the authors anticipated.

In this study, a concept to recover heat from the power losses generated in the working hydraulic system—in order to heat the cabin on an electric mobile machine—was evaluated through model-based simulation. The concept is based on the traditional principle of cabin heat management, where a glycol-water mix—here called transport medium—recovers heat from the ICE and possibly an auxiliary heater and delivers it to a heating core in the cabin. A corresponding version for an electric mobile machine involves multiple heat sources, and is illustrated in fig. 2. Here only one of them is considered, but on the other hand the heat source with the most uncertainties.

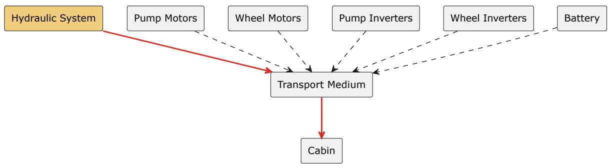

Figure 2: A diagram illustrating the focus area of the paper—the heat loss path from the hydraulic system to the cabin, highlighted with solid red arrows—in the context of an interconnected heat recovery system with several additional potential heat sources marked with dashed arrows.

1.1 Contributions

This paper focus on the working hydraulic system—and specifically the possibilities and challenges of recovering hydraulic heat losses to heat the cabin. A model of a hydraulic heat recovery system is presented, and the simulation results are analyzed and discussed. Both the dynamic behavior typically associated with hydraulic systems in combination with heat recovery, and the heating performance of the cabin are considered.

2 Modeling

The model was created with Modelica using standard components within the DLR Thermofluid Stream (TFS) library [7, 8], and the Modelica Standard Library. The TFS components used to model the fluid circuits are described in detail in [8]. Modelica Standard Library components were used for the control of the model. The selected parameters used within the model components and referred to in this chapter are listed in tab. 1. The simulations were performed using the open-source simulation tool OpenModelica. The main purpose of the model was to evaluate the impact of dynamic heat losses on the cabin air temperature—driven by oil temperature and mass flow—from the working hydraulic system of a mobile machine, when part of the heat flow is harvested and used to heat the cabin. The model shown in fig. 3 is the studied practical implementation of the heat loss path illustrated in fig. 2, and consists of the three main fluid circuits: hydraulic circuit, transport medium circuit, and cabin air supply circuit. A fourth circuit representing an ambient chiller, together with a hysteresis control logic is modeled to limit the hydraulic oil reservoir temperature to 60–70°C.

Table 1: Selected parameters used in the model components and simulations, some of which are subject to a sensitivity analysis, where the value listed in the table represents the selected base value.

Variable	Symbol	Value	Unit
Measured mean flow rate [4]	q_{mean}	2.54×10^{-3}	m^3/s
Measured mean heat flow [4]	$\dot{Q}_{mean}$	35.7×10^3	W
Intensity factor	X_I	1	–
Amplitude factor (heat)	$X_{A_{heat}}$	1	–
Amplitude factor (flow)	$X_{A_{flow}}$	1	–
Phase angle offset (heat)	φ_{heat}	0	rad
Heat loss frequency	f_h	0.1	Hz
Transport medium mass flow rate	$\dot{m}_{tm}$	0.186	kg/s
Cabin air mass flow rate	$\dot{m}_c$	0.11	kg/s
Overall Conductance (hydraulic)	UA_h	300	W/K
Overall Conductance (cabin)	UA_c	125	W/K
Reservoir volume (hydraulic)	V_h	0.34	m^3
Reservoir volume (transport)	V_{tm}	0.001	m^3
Cabin volume	V_c	1	m^3
Ambient temperature	T_{amb}	-15	°C
Simulation stop time	t_{stop}	3600	s
Simulation interval		0.1	s

The hydraulic circuit is modeled to represent the low-pressure return line of the working hydraulic system, transporting the heat losses to the ambient chiller and back to the hydraulic reservoir with the volume V_h. The heat losses from the working hydraulic system are modeled as a lumped model consisting of a pump and a conduction element. The pump is following a mass flow reference, and the conduction element produces heat according to a heat flow reference. The reference signals, y, in both cases are sine waves, here defined as eq. 1, with an offset value C_q and C_Q according to eq. 2 and 3. X_I is used as an intensity factor between 0–1 representing the degree of operating utility, where 1 is the highest utility representing 100%. The sine wave shape is chosen as model input because of its similarity with how multiple hydraulic cylinder stroke positions moves back and forth during an excavating cycle, creating continuous alternating flow rates and heat losses, while maintaining the simplicity of the model. The flow rate q_{mean} and heat flow $\dot{Q}_{mean}$ are based on measured average values during a high-utility excavating cycle from previous work [4]—here referred to as intensity factor $X_I = 1$—and can be found in tab. 1. The amplitude A of the sine waves are controlled by the use of amplitude factors $X_{A_{heat}}$ and $X_{A_{flow}}$, according to eq. 4. The frequency f_h is always the same for the two sine waves. The phase angle of the heat flow sine wave φ_{heat} can be adjusted in the positive direction relative to the flow sine wave, to model a transport delay of the oil temperature increase. The conduction element uses the sine wave heat flow reference directly as input, while the pump component creating the flow in the hydraulic circuit needs a P-controller from mass flow rate into an angular velocity control signal. Before reaching the ambient chiller, the hydraulic fluid is passing through a heat exchanger to harvest

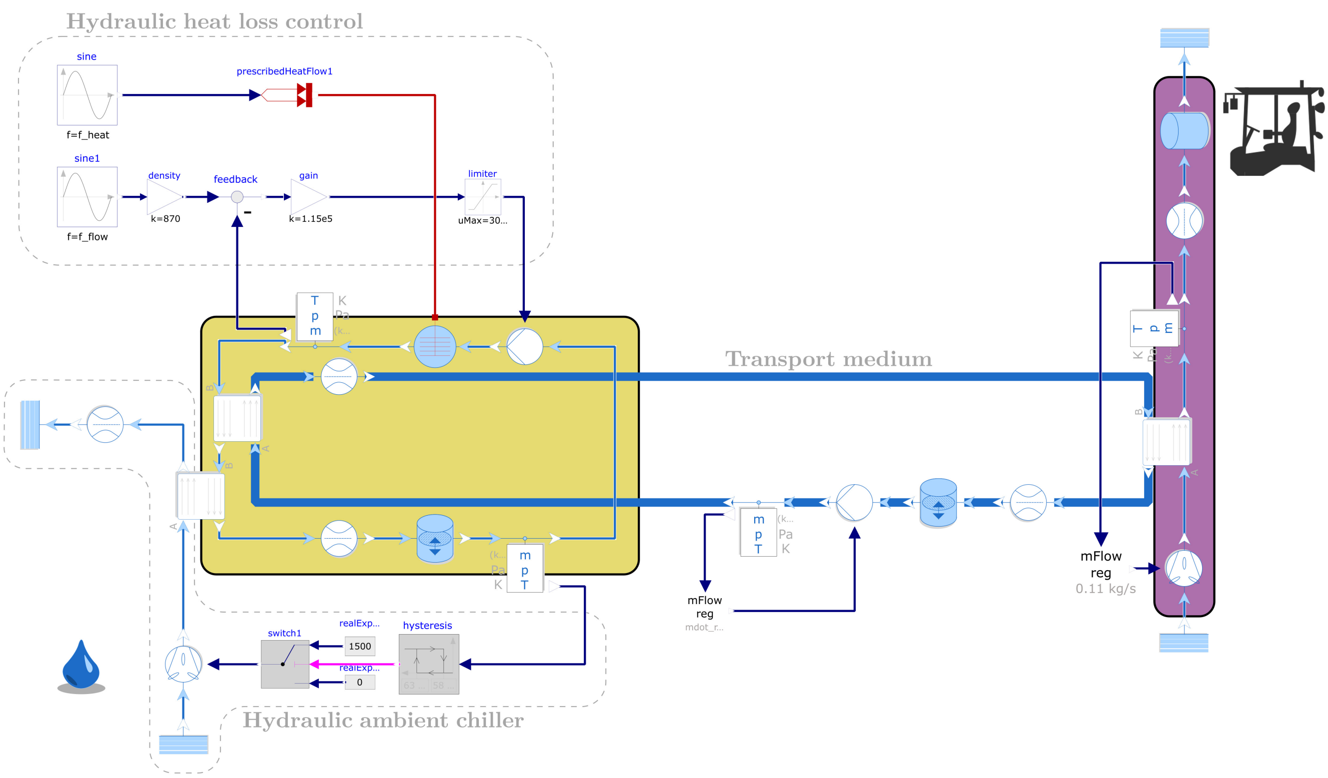

Figure 3: Modelica model of the studied hydraulic heat loss recovery system, composed of a hydraulic fluid circuit highlighted in the yellow zone, a transport medium circuit highlighted in thick blue lines, and a cabin air supply circuit highlighted in the purple zone. Additionally, a hydraulic ambient chiller circuit highlighted with dashed lines makes sure to maintain the oil reservoir temperature within 60–70°C. The fluid circuits are modeled with TFS standard components explained in [8]. The control of the TFS components are modeled with the Modelica Standard Library.

heat losses to the cabin via a transport medium.

$$y = A \sin(2\pi f_h t + \varphi) + C \tag{1}$$

$$C_q = X_I q_{mean} \tag{2}$$

$$C_Q = X_I \dot{Q}_{mean} \tag{3}$$

$$A = X_A C \tag{4}$$

The transport medium circuit in this concept has the purpose of collecting heat losses from different subsystems of a vehicle and transporting the heat to the cabin, as shown in fig. 2. In this model only one subsystem, the hydraulic system, is modeled. Similar to the hydraulic circuit a flow is generated with a pump component, controlled to maintain a fixed mass flow rate of glycol-mixed water, $\dot{m}_{tm}$. The heat is collected with a heat exchanger component based on the εNTU-method, parametrized with overall heat transfer coefficient U and the conductive surface area. Here, these two heat exchanger properties are combined as the overall conductance UA and can be found in tab. 1. A second heat exchanger is transferring the heat from the transport medium to the cabin air. A reservoir component with volume V_{tm} is acting as flow source and sink.

The cabin air supply circuit is modeled with a fan maintaining a constant mass flow rate of air, $\dot{m}_c$, from a source with a preset temperature value of T_{amb}. A volume component of the size V_c is used to model the actual cabin. The outlet of the cabin volume is the point of where the temperature dynamics are evaluated in chapter 3, and is treated as the actual temperature in the cabin. The air media used is a dry air model.

The media models used in the hydraulic circuit and the transport medium circuit are both table based. The model for glycol-mixed water used in the transport medium circuit is the Glycol47 model available in the TFS library. The hydraulic oil model is the table of assumed values in tab. 2.

Table 2: Table-based media model of a hydraulic oil used in this model. The table structure is reused from the glycol-water model Glycol47 in the TFS library.

Temp °C	Density kg/m^3	Heat Capacity J/kgK	Conductivity W/mK	Viscosity Pa s	Vapor Pressure Pa
-40	896	1700	0.13	0.27	0.0001
-20	888	1800	0.13	0.18	0.0005
0	880	1900	0.13	0.11	0.001
20	872	2000	0.13	0.061	0.005
40	864	2100	0.13	0.04	0.01
60	856	2200	0.12	0.027	0.05
80	848	2300	0.12	0.021	0.1
100	840	2400	0.12	0.017	0.5
120	832	2500	0.11	0.014	1
140	824	2600	0.11	0.012	2
150	820	2650	0.10	0.011	3

3 Results

This section presents the results from the simulations made with the presented model. The results are divided into the two focus areas dynamic response and heating performance. Figures 4– 9 illustrate different sensitivity analyses of the cabin temperatures as oscillating peak-to-peak values versus model parameters. The cabin heating performance is shown in fig. 10 and 11.

3.1 Dynamic Response

Figure 4 shows three different sensitivity analyses. The green and orange lines show the resulting peak-to-peak temperatures when only one of the two sine wave amplitudes is varied while the other remains at zero. The blue line shows how the peak-to-peak temperature of the cabin air changes when both input amplitudes are changed simultaneously. It can be seen that as long as the amplitude factor X_A for both sine wave signals increases equally, the peak-to-peak temperature of the cabin air does not change significantly until the amplitude reaches its higher end point. The same point is also selected as base value for the other sensitivity analysis below.

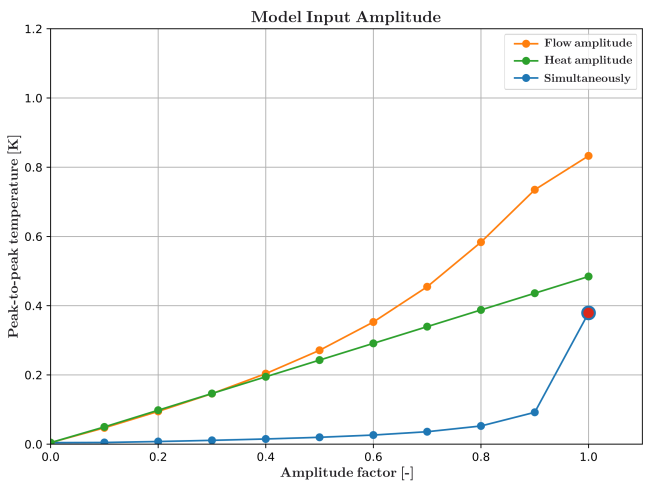

Figure 4: Sensitivity analysis of cabin air peak-to-peak temperature on the vertical axis, with amplitude factors $X_{A_{heat}}$ and $X_{A_{flow}}$ as input parameters on the horizontal axis. Green and orange lines show the cabin peak-to-peak temperature when the heat loss and flow rate amplitudes are changed separately, with the other amplitude factor set to zero. The blue line shows the peak-to-peak temperature when the two amplitude factors are changed simultaneously. The red dot marks the base value selected for the model.

Figure 5 shows how the sine wave frequency affects the peak-to-peak value of the cabin air temperature. It is observed that low frequencies have a significant impact on the peak-to-peak temperature.

Figure 6 shows how the phase angle offset between the flow sine wave and the heat loss sine wave affects the peak-to-peak temperature of the cabin air. It can be noted that the selected base value of the phase angle offset in the model is $\varphi_{heat} = 0\,\text{rad}$.

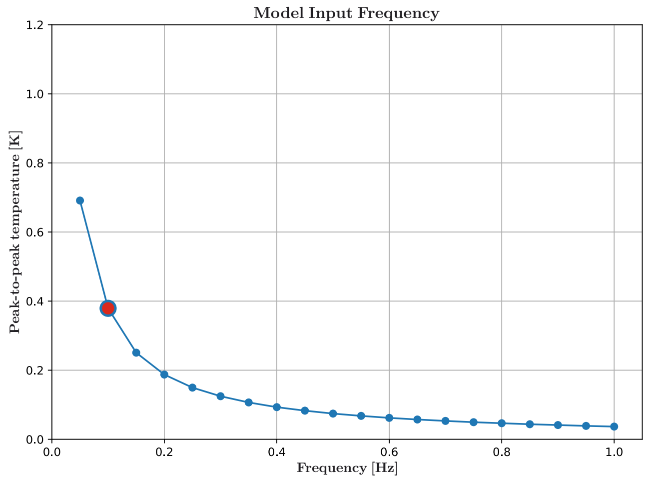

Figure 5: Sensitivity analysis of cabin air peak-to-peak temperature on the vertical axis, with heat loss frequency f_h as input parameter on the horizontal axis. The red dot marks the base value selected for the model.

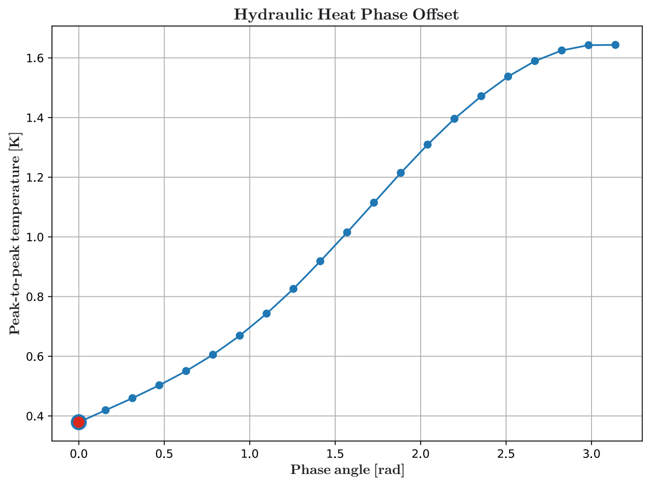

Figure 6: Sensitivity analysis of cabin air peak-to-peak temperature on the vertical axis, with heat flow phase angle offset φ_{heat} as input parameter on the horizontal axis. The red dot marks the base value selected for the model.

The transport medium mass flow rate sensitivity is shown in fig. 7, and the cabin air mass flow rate in fig. 8. It is observed that changing the mass flow rate has opposite effects on the peak-to-peak temperatures.

Finally, fig. 9 shows how the overall conductance UA affects the temperature peak-to-peak values for both the hydraulic and the cabin heat exchanger. It is noted that the cabin heat exchanger is more sensitive to changes in overall conductance than the hydraulic heat exchanger.

3.2 Heating Performance

Figure 10 shows the heat-up time of the cabin for different hydraulic tank volumes after a cold start at –15°C, with the other model parameters set to their base values. The cabin air

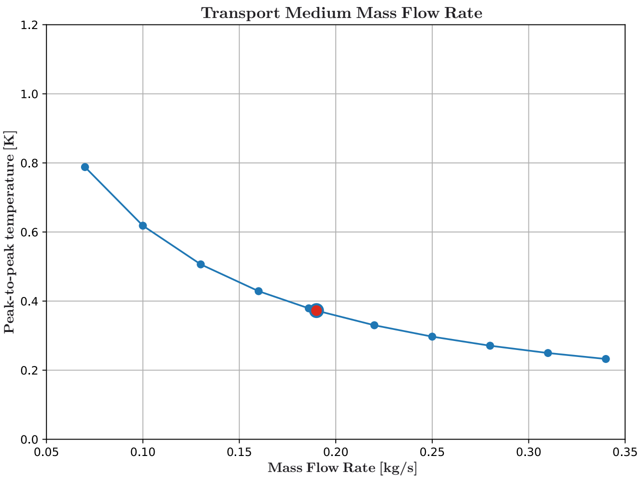

Figure 7: Sensitivity analysis of cabin air peak-to-peak temperature on the vertical axis, with varying transport medium mass flow rate $\dot{m}_{tm}$ as input parameter on the horizontal axis. The red dot marks the base value selected for the model.

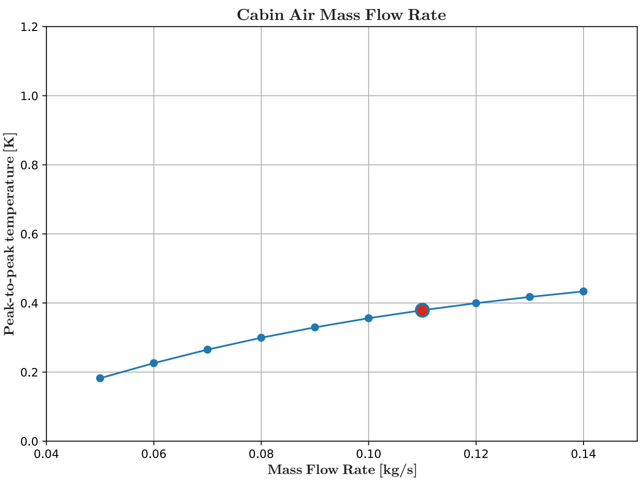

Figure 8: Sensitivity analysis of cabin air peak-to-peak temperature on the vertical axis, with varying cabin air mass flow rate $\dot{m}_c$ as input parameter on the horizontal axis. The red dot marks the base value selected for the model.

temperature is limited by the maximum oil temperature, which in turn is limited by the ambient chiller. The tank volume of 10 liters gives a heat-up time for the cabin that is 12 times faster than for a tank volume with 350 liters. It can also be noted that the heat up time for the cabin from –15°C to 20°C with the 350 liter hydraulic tank is approximately 18 minutes.

Figure 11 shows the cabin air temperature during a cold start as a result of different values of the intensity factor X_I, with the other parameters set to their base values. Even though the graph ends after 60 minutes, the temperatures keep increasing up to 33°C for all intensity factors except for $X_I = 0.1$.

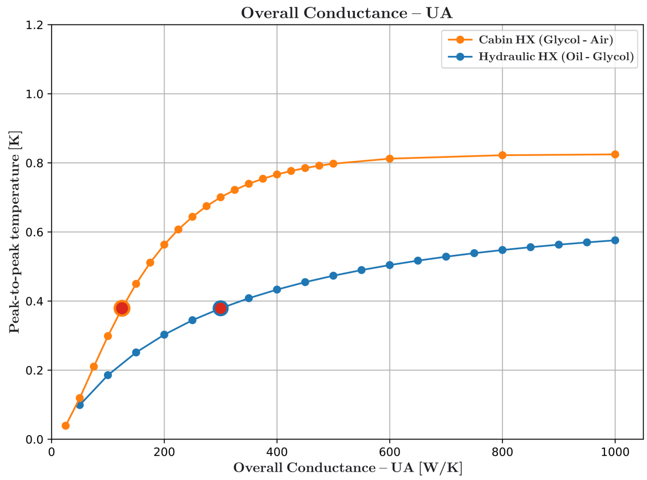

Figure 9: Sensitivity analysis of cabin air peak-to-peak temperature on the vertical axis, with varying overall conductance of the hydraulic and cabin heat exchanger UA_h and UA_c as input parameters on the horizontal axis—one heat exchanger at a time, with the other at base value. The red dots mark the base values selected for the model.

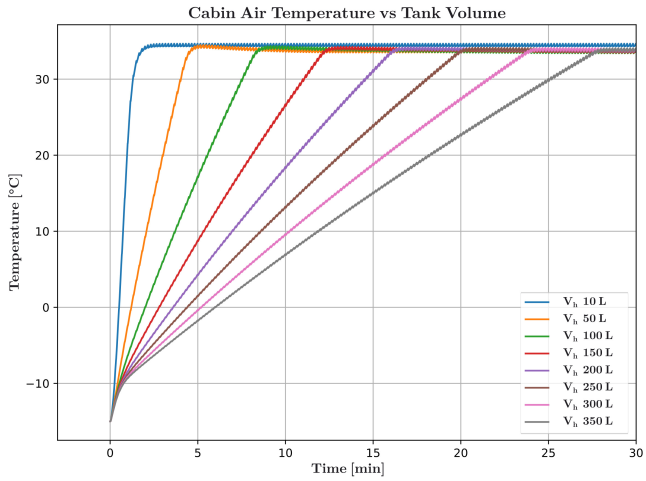

Figure 10: Cold start performance of the simulated cabin air temperature is shown on the vertical axis starting from –15°C, with simulation time on the horizontal axis. Each curve represents a different value of the hydraulic tank volume V_h.

4 Discussion

The purpose of this paper was to study the possibilities and challenges of recovering waste heat from a working hydraulic system to warm the intake air supply of a cabin by utilizing a heat exchanger on the hydraulic low-pressure return line. Additionally, to investigate and to learn more about important parameters to consider if a such heat recovery concept would be implemented in a final product. Due to the dynamic nature of working hydraulic systems, and the challenge to practically measure these losses in real time, an attempt to create a model and simulate a heat recovery system was presented and studied.

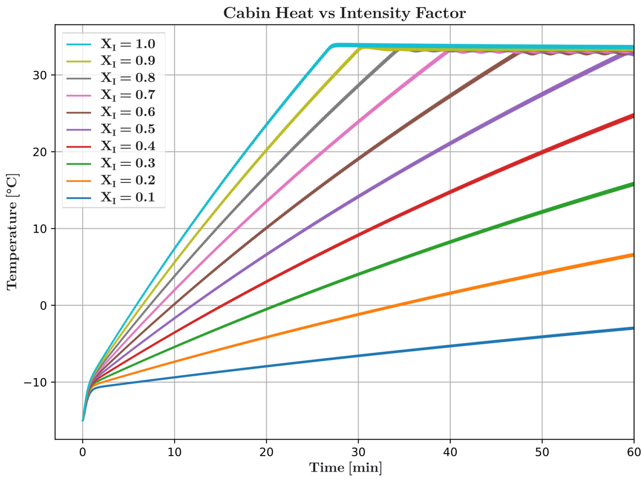

Figure 11: Cold start performance of the simulated cabin air temperature is shown on the vertical axis starting from –15°C, with simulation time on the horizontal axis. Each curve represents a different value of the intensity factor X_I, corresponding to excavating utility levels from 10–100%.

Overall, the findings suggest that harnessing heat from an operational hydraulic system to warm a cabin is a promising strategy. Even though the sensitivity analyses show us that unknown variables such as hydraulic amplitudes, frequency and phase offset affects the peak-to-peak temperature variation in the cabin significantly, there are ways to mitigate these variations such as active temperature control. Additionally, the model used in this paper is quite ideal, with the primary focus of catching the dynamic response. Masses and passive cooling entities exposed to ambient temperatures that occurs in a physical system will likely act as a filter on the dynamic heat flow. Looking back at fig. 2, the working hydraulic system is only one out of several other subsystems, meaning that a heat flow with dynamic behavior can possibly be mixed with more continuous heat flows before reaching the cabin. An active control of the cabin heating and ventilation system could possibly deal with fluctuations in the magnitude of what has been presented here. Finally, the peak-to-peak temperature with the current set of model parameters are almost equal to the human-detectable temperature deviations studied by [5], which further suggests that mitigating measures can be needed.

The heat recovery possibilities and cabin heating performance shown in fig. 10 are promising, however, additional parameter adjustment and validation is recommended to confirm their reliability. On the other hand, by making a simple comparison of the rate of temperature increase of the hydraulic oil tank between the simulation results from $V_h = 350\,\mathrm{L}$, and a previous measurement on a system with a similar tank volume, the simulated result is only 12% faster. The simulation result is based on the highest intensity factor—which was also the case in fig. 1—and is not the most common operating point. Assuming that intensity factor $X_I = 0.5$ is the most common operating point in average, the time it takes for the cabin to reach 20°C is almost 40 minutes, as can be seen in fig. 11. With that in mind, it can be motivated to look at downsizing the hydraulic tank volume to faster reach operation temperatures. For example, three cylinders required for the most basic digging motion requires a differential volume of roughly 35 liters, even though the hydraulic tank holds hundreds of liters. Due to the variety of hydraulic functions and operating scenarios of a machine, it might not be possible to downsize the tank. However, there could still be a reason to introduce a tank solution such that only a fraction of the total stored volume is utilized and heated until more is needed. Essential functionality such as air bleeding and oil filtration might however prevent or complicate such solutions to be implemented.

From the results it seems like the heat losses from the hydraulic system alone can sufficiently heat the cabin, which might be the case in some specific operating modes. There are, on the other hand, numerous situations where a mobile machine does not use the hydraulic system in the continuous manner required to produce the amount of heat presented in this paper—for example, transportation along a road from one work site to another, or idle-like tasks such as moving and holding heavy objects. This is one of the motivations behind an interconnected heat recovery system like the one illustrated in fig. 2. However, the working hydraulic system allows the direct heat recovery principle for electric mobile machines to cover the cabin heat demand during hydraulic operation, even under lower intensities. During low intensity transportation the available waste heat might not cover the cabin demand, which (with a bit of imagination) is indicated in fig. 1. In some of those cases—given that the machine was hydraulically operated before—the hydraulic tank could serve as a thermal storage device. In contrast to electric passenger cars, the amount of available waste heat is not always the issue for electric mobile machines—it is how to recover it.

5 Conclusions

Working hydraulic heat recovery may not always be exclusively sufficient to heat the cabin, but it offers a good heat source despite its dynamic characteristics. Technical solutions to allow the hydraulic oil heat-up time to be shortened can improve the heating performance in the cabin.

Acknowledgement

This research was funded by the Swedish Energy Agency (Energimyndigheten) with grant number P2023-00596.

References

[1] Zhen Tian, Bo Gu, Wenzhong Gao, and Yuan Zhang. Performance evaluation of an electric vehicle thermal management system with waste heat recovery. *Applied Thermal Engineering*, 169:114976, March 2020.

[2] Gabriele Leoncini, Ronan Mothier, Benoît Michel, and Marc Clausse. A review on challenges concerning thermal management system design for medium duty electric vehicles. *Applied Thermal Engineering*, 236:121464, January 2024.

[3] Sagar Singh, Mark Jennings, Sunil Katragadda, Judy Che, and Nenad Miljkovic. System design and analysis methods for optimal electric vehicle thermal management. *Applied Thermal Engineering*, 232:120990, September 2023.

[4] Fabian Lagerstedt, Samuel Kärnell, Marcus Rösth, and Liselott Ericson. Analysis of opportunities for integrated thermal management on battery powered mobile machines. In *Global Fluid Power Society PhD Symposium, GFPS 2024*, 2024. submitted.

[5] Laura Battistel, Andrea Vilardi, Massimiliano Zampini, and Riccardo Parin. An investigation on humans' sensitivity to environmental temperature. *Scientific Reports*, 13(1):21353, December 2023.

[6] Zhengzhao Gu, Kewen Feng, Lei Ge, and Long Quan. Dynamic modeling and optimization of organic Rankine cycle in the waste heat recovery of the hydraulic system. *Energy*, 263:125673, January 2023.

[7] Dirk Zimmer. Robust object-oriented formulation of directed thermofluid stream networks. *Mathematical and Computer Modelling of Dynamical Systems*, 26(3):204–233, 2020.

[8] Dirk Zimmer, Michael Meißner, and Niels Weber. The dlr thermofluid stream library. *Electronics*, 11(22), 2022.